Correlations between dual-phase ^{18}F-FDG uptake and clinicopathologic and biological markers in predicting the aggressiveness of breast cancer

Hayato Kaida[1] MD,
Koichi Azuma[2] MD,
Uhi Toh[3] MD,
Akihiko Kawahara[4] PhD,
Eiji Sadashima[5] PhD,
Satoshi Hattori[6] PhD,
Jun Akiba[4] MD,
Nobuhiro Tahara[7] MD,
Axel Rominger[8] MD,
Kazunari Ishii[1] MD,
Takamichi Murakami[1] MD,
Masatoshi Ishibashi[9] MD

1. Department of Radiology, Kindai University Faculty of Medicine, Osakasayama City, Osaka 589-8511, Japan
2. Division of Respirology, Neurology and Rheumatology and Department of Internal Medicine, Kurume University School of Medicine, Kurume City, Fukuoka, 830-0011, Japan
3. Department of Surgery, Kurume University School of Medicine, Kurume City, Fukuoka, 830-0011, Japan
4. Department of Diagnostic Pathology, Kurume University Hospital, Kurume City, Fukuoka, 830-0011, Japan
5. Shin-Koga Hospital, Medical Corporation Tenjinkai, Kurume City, Fukuoka, 830-8577, Japan
6. Biostatic Center, Kurume University School of Medicine, Kurume City, Fukuoka, 830-0011, Japan
7. Division of Cardiovascular Medicine and Department of Internal Medicine, Kurume University School of Medicine, Kurume City, Fukuoka, 830-0011, Japan,
8. Department of Nuclear Medicine, Ludwig Maximilians University Munich, Munich, 81377, Germany
9. Division of Nuclear Medicine, PET Center, Department of Radiology, Fukuoka Tokushukai Hospital, Kasuga City, Fukuoka, 816-0864, Japan

Corresponding author:
Hayato Kaida M.D.
Department of Radiology, Kindai University Faculty of Medicine
Ohnohigashi 377-2, Osakasayama City, Osaka, 589-8511, Japan
Telephone: +81-(72)-366-0221
FAX: +81-(72)-367-1685
kaida@med.kindai.ac.jp

Abstract

Objective: To assess the correlations between dual-phase fluorine-18 fluorodeoxyglucose (^{18}F-FDG) uptake and clinicopathological and immunohistochemical prognostic factors in patients with surgically resected breast cancer stage I-III. **Subjects and Methods:** We retrospectively analyzed the cases of 105 patients. We calculated the maximum standardized uptake value (SUVmax) at 85min (SUV1), SUVmax at 125min (SUV2) and the retention index [RI]. Spearman's rank correlation test, the Kruskal-Wallis test and receiver operating characteristic (ROC) analysis were performed to assess the association between ^{18}F-FDG uptake and the clinicopathological and immunohistochemical factors: glucose transporter-1 (Glut-1), estrogen receptor alpha (ERα), ERβ, progesterone receptor (PR), human epidermal growth factor 2 (Her2), mammalian target of rapamycin (mTOR), and P70S6kinase (P70S6). **Results:** The SUV1 and SUV2 values were correlated with Glut-1, pathological tumor size, ERα negativity, and pathological stage (all P values were <0.05), but not with mTOR, P70S6, ERβ, PR, Her2 or other factors. The SUV1 and SUV2 in the triple negative subtype were significantly higher than those of the hormone receptor-positive subtype (P<0.05). The RI was associated with pathological tumor size alone. In the ROC analysis of Glut-1, the areas under the curve for SUV1 and SUV2 were significantly larger than for RI (SUV1, P=0.032, SUV2, P=0.022). **Conclusion:** Glucose transporter-1, estrogen receptor alpha negativity and nuclear grade might affect the high ^{18}F-FDG uptake in breast cancer. The SUVmax might be more useful than the RI for predicting the Glut-1 expression and the aggressiveness of breast cancer.

Introduction

Breast cancer is the leading cause of cancer death among females worldwide, with an estimated 1.7 million cases and 521,900 deaths in 2012 [1]. Breast cancers are biologically heterogeneous tumors, and estrogen receptor (ER), progesterone receptor (PR), and human epidermal growth factor 2 (Her2) have been used to decide the management of adjuvant therapy. Triple-negative breast cancer (TNBC) has a poor prognosis, and the recurrence rate of TNBC is significantly higher than those of Her2-positive cancer or hormone receptor (HR)-positive cancer [2]. It is important for us to understand the clinicopathological risk factors of breast cancer in order to determine the optimal patient management and to improve the prognosis of breast cancer patients.

Fluorine-18 fluorodeoxyglucose positron emission tomography/computed tomography (^{18}F-FDG PET/CT) is useful for estimating staging, local recurrence and distant metastasis, and for tracking the effects of therapy for breast cancer [3, 4]. Dual-phase ^{18}F-FDG PET imaging has been used to differentiate benign and malignant lesions, and it provides more information about ^{18}F-FDG accumulation in a lesion than single-point imaging; a high retention index (RI) calculated from the percent change in the maximum standardized uptake value (SUVmax) between early and delayed images indicates a high possibility of malignancy in breast cancer patients [5, 6]. Dual-phase ^{18}F-FDG PET imaging has also been used to predict the prognosis of malignant tumors such as lung cancer, pancreas cancer and rectal cancer [7-9]. The relationships between clinicopathological risk factors and parameters such as the RI and the SUVmax have been investigated, but the relationships between clinicopathological risk factors and these markers are diverse and not fully agreed upon.

Glucose transporter-1 (Glut-1) is related to the ^{18}F-FDG uptake mechanism of malignant tumors. The mammalian target of rapamycin (mTOR) signal pathway (which is upstream of Glut-1 and regulates the Warburg effect) is related to Her2 expression, and mTOR contri-

butes to the tumor progression of breast cancer [10]. However, to our knowledge, the relationships between ^{18}F-FDG uptake and Glut-1 and HR expressions and the Her2/mTOR signal pathway examined in a dual-phase PET study based on molecular pathology have not been reported. The aim of the present study was to determine the correlations between dual-phase ^{18}F-FDG uptake and immunohistochemical markers and the correlations between dual-phase ^{18}F-FDG uptake and clinicopathological prognostic factors in patients with surgically resected breast cancer.

Subjects and Methods

Patients

This was a retrospective study of 105 female breast cancer patients who underwent an ^{18}F-FDG PET/CT examination and complete surgical resection in the period from November 2008 to October 2011. None of the patients had undergone neo-adjuvant chemotherapy before surgery. Histopathological specimens were obtained from surgically resected samples.

Our inclusion criteria are shown in Figure 1. Our final study population consisted of 76 female patients with a median age of 60 (range 37-91) years. The clinical and histopathological stages were based on the International Union against Cancer (UICC 2002) tumor-node-metastasis (TNM) classification [11]. The study protocol was conducted according to the Declaration of Helsinki. The study protocol was approved and informed consent from each patient was waived by the Kurume University School of Medicine Institutional Review Board (research number 10297).
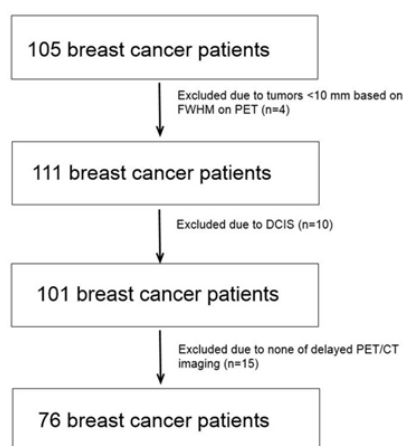
Figure 1. The flow diagram shows the inclusion criteria on this study. The patients whose tumors were <10mm based on the full width at half maximum (FWHM) on PET (n=4) and those whose histopathological finding was ductal carcinoma in situ (DCIS) (n=10) were excluded. Fifteen patients who could not undergo delayed-phase ^{18}F-FDG PET/CT were also excluded.

^{18}F-FDG PET/CT imaging acquisition

An integrated full-ring PET/CT scanner (Gemini-GXL 16; Philips Medical Systems, Cleveland, OH, USA) was used for data acquisition. Before the ^{18}F-FDG injection, the patient fas-

ted for 4hr. The intake of liquids without sugar content was permitted. Prior to the examination, the patient drank 500 mL of water to accelerate renal ^{18}F-FDG elimination. The patients' median blood glucose level was 108mg/dL (range 74-130mg/dL). The patients were administered a mean 295MBq (range 82-434) dose of ^{18}F-FDG via the antecubital vein. All patients rested quietly for approx. 60min after the ^{18}F-FDG intravenous injection.

First, whole-body PET/CT image in the supine position was performed. A non-contrast full-dose CT scan was acquired using the following parameters: 200mAs, 120 kV, 0.75 sec/tube rotation, 3mm slice thickness, 940mm scan length and 40sec data acquisition time. The CT scan was acquired during breath-holding in the normal expiratory position. The CT data were used for attenuation correction and lesion localization. Positron emission tomography scans were acquired with a time of 2min 30sec per bed position using a three-dimensional (3D) acquisition mode. After both the transmission of CT and emission images were obtained, the images were reconstructed using the standard normal reconstruction protocol based on the 3D line-of-response row-action maximum likelihood algorithm with which the PET/CT scanner is equipped. Whole-body PET/CT image from the level of the auditory meatus to the mid-thigh resulted in an acquisition time of approx. 20min.

As soon as the whole-body PET/CT imaging was achieved, prone breast PET/CT imaging was performed at approx. 85 min after ^{18}F-FDG injection. The prone breast PET/CT imaging included the mammary gland alone, with an acquisition of one or two emission scans. The patient was in the prone position with her arms at her sides. For positioning, a foam cushion on the scanner table was adopted with holes that allowed the patient's breasts to be unconstrained [12]. Prone breast PET/CT image resulted in an acquisition time of approx. 7min.

Delayed prone breast PET/CT imaging was performed at approx. 125min after the administration of ^{18}F-FDG, using identical parameters. All 76 breast cancer patients underwent both supine and prone ^{18}F-FDG PET/CT imaging.

^{18}F-FDG-PET/CT image analysis

On a workstation (Sun Microsystems, Santa Clara, CA), the volumetric region of interest (VOI) was drawn over the entire area of abnormal focal uptake on the primary lesion to include a large amount of radioactivity semiautomatically. The SUVmax value of breast cancer-associated accumulation was calculated at approx. 85min (SUV1) and at approx. 125min (SUV2) following the administration of ^{18}F-FDG, and recorded automatically. The retention index (RI) was calculated as follows: $RI(\%)=[(SUV2-SUV1)/SUV1]\times100$.

Immunohistochemical staining

Immunohistochemical staining (IHC) was performed for all 76 patients. Paraffin-embedded tissue samples were cut at 4μm examined on a coated slide glass and labeled with the following antibodies using the automated slide preparation system BenchMark XT (Ventana Automated Systems, Tucson, AZ) and a Bond-III autostainer (Leica Microsystems, Newcastle, UK): Glut-1 (1:100, Thermo Scientific, Rockford, IL), ERα (ready to use; Ventana), ERβ (1:100, Abcam, Cambrid-

ge, MA), PR (ready to use; Ventana), Her2 (ready to use; Ventana), mTOR (1:100, Cell Signaling Technology, Danvers, MA), and p70S6 (1:100, Cell Signaling Technology).

Briefly, each slide was heat-treated for 30min with Ventana's cell conditioning 1 (CC1) retrieval solution at 95°C. For Glut-1, Her2, ERα, PR and p70S6, we used the BenchMark XT system and the streptavidin biotin complex method with 3,3' diaminobenzidine (DAB) as the chromogen (Ventana Ultra View DAB detection kit). For ERβ and mTOR, the Bond-III system was used with a Refine polymer detection kit (Leica Microsystems) with DAB as the chromogen. Briefly, ERβ and mTOR were heat-treated using epitope retrieval solution 2 (pH9.0) for 20min at 99°C, and incubated with each antibody for 30min at room temperature.

Evaluation of clinicopathological markers and IHC findings

We performed a scoring analysis to evaluate the expressions of Glut-1, Her2, mTOR, and p70S6. The IHC for these antibodies was evaluated as positive according to the cytoplasm and/or membrane reactivity. The intensity of cytoplasm/membrane staining was scored as follows: no staining, 0; weak staining of <10% cancer cells, 1+; moderate staining of ≥10% to 50% cancer cells, 2+; strong staining of >50% cancer cells, 3+. The scores 2+ and 3+ were considered to indicate positivity.

The extent of staining of ERα, ERβ, and PR proteins was classified based on the percentage of cells with strongly stained nuclei: ≥10% indicated that a gland was positive, and ≤9% indicated that a gland was negative. When the IHC staining result of Her2 was +3, or when the IHC result of Her2 was +2 and the value of gene amplification using fluorescence in-situ hybridization (FISH) was over 2.0, Her2 was defined as positive.

The breast cancer subtypes were classified as follows: Progesterone receptor , ER and Her2 expression negative was the triple-negative (TN) subtype. All other breast cancer sub-types were classified as follows; HR (−) Her2 (+) subtype (PR- and/or ER-negative, Her2-positive), hormone receptor-positive group [HR (+) subgroup (PR- and/or ER-positive, Her2-positive or -negative)].

Histological grading was determined on the basis of the tubular structure, nuclear pleomorphism, and mitotic count following the modified criteria of Bloom and Richardson; in cases of invasive carcinoma, the grades range from I to III [13]. The pathological tumor size (p-tumor size) was estimated by measuring the maximum diameter of the tumor invasive component (in mm). For the pathological T stage (pT), we divided the total patient population (n=76) into two groups: pT1 (<2cm) and pT2-4 (≥2cm). Pathological lymph nodal (pN) status was categorized as nodal metastasis-positive or nodal metastasis-negative.

We also divided the patient population into a premenopausal group and a postmenopausal group. Menopause was defined as cessation of menstrual period that had lasted more than 12 months. All IHC results were evaluated by two experienced observers who were blind to the condition of the patients.

Statistical analysis

The Spearman rank correlation test was used for all analyses. We performed a receiver operating characteristic (ROC) analysis to examine which ^{18}F-FDG PET parameters reflected the immunohistochemical markers and clinicopathological prognostic factors. Association between ^{18}F-FDG PET parameters and the subtype of hormone and Her2 status or association between Glut-1 expression and the subtype of hormone and Her2 status were examined by Kruskal-Wallis test and Fisher exact test. The statistical analyses were performed using SAS ver. 9.4 (SAS, Cary, NC). A P-value <0.05 was considered significant.

Results

Patients' characteristics
Patient's characteristics are shown in Tables 1 and 2.

Table 1. *The characteristics of 76 breast cancer patients.*

Clinical and Laboratory	Number
Menopause	22
Post menopause	54
pStage I	34
>> IIA	31
>> IIB	9
>> III	2
Histopathological type	
IDC	60
Mucinous carcinoma	5
Medullary carcinoma	3
Micropapillary carcinoma	3
Invasive lobular carcinoma	2
Apocrine carcinoma	2
Invasive high grade carcinoma with acellular zone	1
pT stage	
pT1	44
pT2-4	32

pN	
Positive	19
Negative	57
NG I	44
>> II	17
>> III	15
ER α	
Positive	57
Negative	19
ER β	
Positive	20
Negative	56
PR	
Positive	43
Negative	33
Her2	
Positive	55
Negative	21
Subtype	
HR (+) subtype	57
HR (-) Her2 (+) subtype	10
TN subtype	9

pStage; pathological Stage, IDC; invasive ductal carcinoma, NG; nuclear grade, ER; estrogen receptor, PR; progesterone receptor, Her2; human epidermal growth factor-2, pT; pathological T stage, pN; pathological N status, HR (+) subtype; hormone receptor positive subtype, HR (-) Her2 (+) subtype; hormone receptor negative, human epidermal growth factor-2 positive subtype, TN subtype; triple negative subtype.

Table 2. *The result of immunohistochemical staining of Glut-1, mTOR and P70S6 in breast cancer patients.*

| Molecular markers	score 0	score 1	score 2	score 3
Glut-1	17	30	19	10
mTOR	13	21	22	20
p70S6	0	13	39	24

Glut-1; glucose transporter-1, mTOR; mammalian target of rapamycin, p70S6; P70S6 kinase

The primary tumors of all 76 patients were ^{18}F-FDG uptake-positive on ^{18}F-FDG PET/CT. The median SUV1 of the patients was 3.82 (the 25th and 75th percentiles of the interquartile range [IQR]: 2.42-6.16). The median SUV2 was 4.33 (IQR 2.56-6.53), and the median RI was 10.95% (IQR -1.24-23.43). The median p-tumor size was 18.5mm (IQR 15-25).

The correlations between ^{18}F-FDG uptake and clinicopathological and biological markers

The correlations between the ^{18}F-FDG uptake parameters and the immunohistochemical and clinicopathological prognostic factors are summarized in Table 3.

Standardized uptake value-1 and SUV2 were both positively correlated with Glut-1, and they were both significantly negatively correlated with ERα. SUV1 and SUV2 were not correlated with mTOR, P70S6, ERβ, PR or Her2. The RI was not correlated with any of the immunohistochemical markers. Both SUV1 and SUV2 were significantly positively correlated with p-tumor size, NG, nuclear atypia (NA), nuclear mitosis (NM), and pathological Stage (pStage), but not with age, menopausal status, histopathological type, p-N status, or p-T stage. The RI was positively correlated only with the p-tumor size. A representative sample of PET/CT images and IHC is shown in Figure 2. Regarding the association between breast cancer subtypes and ^{18}F-FDG uptake parameters, there were significant differences between the breast cancer subtypes and both SUV1 and SUV2 (SUV1: P=0.018, SUV2: P=0.0206). The SUV1 and SUV2 in the TN subtype were significantly higher than those of the HR-positive subtype (SUV1: P=0.018; SUV2: P=0.026). There were no significant differences in the RI values between the TN subtype and other subtypes (P= 0.512) (Figure 3).
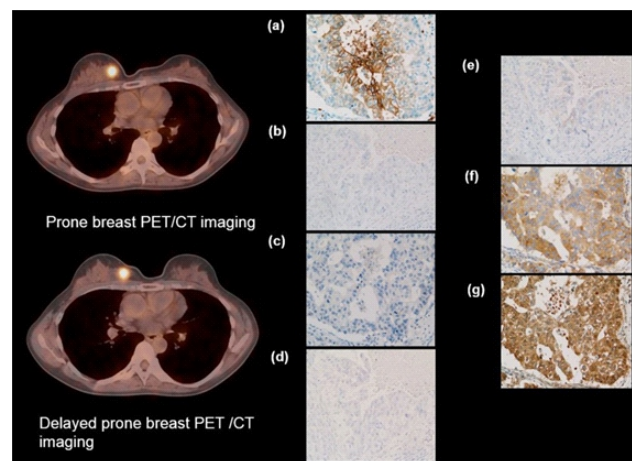
Figure 2. A 53 years old woman with breast cancer (pT1N0M0 stage IA; p-tumor size 15mm, Ng2). The SUV1, SUV2 and RI were 10.1%, 13.8% and 34.92%, respectively. The scores of Glut-1 (a), mTOR (f), and p70S6 (g) expressions were 3, 2 and 2, respectively. The expressions of ERα (b), ERβ (c) PR (d), and Her2 (e) were all negative.

Comparison of ^{18}F-FDG PET parameters by ROC analysis

The ROC curves of ^{18}F-FDG PET parameters Glut-1, ERα, pStage and NG are shown respectively (Figures 4, 5). The area un-

Table 3. The correlation between ^{18}F-FDG uptake and clinicopathologic andimmunohistochemical prognostic factors

|	SUV1	P value	SUV2	P value	RI	P value
Glut-1	r=0.411	<0.001	r=0.398	<0.001	r=0.130	0.262
Her2	r=0.025	0.832	r=0.046	0.691	r=0.041	0.726
mTOR	r=-0.134	0.25	r=-0.086	0.459	r=0.068	0.525
p70S6	r=-0.064	0.583	r=-0.046	0.692	r=0.068	0.557
ERα	r=-0.282	0.014	r=-0.293	0.01	r=-0.132	0.255
ERβ	r=-0.035	0.761	r=-0.037	0.752	r=0.002	0.981
PR	r=-0.106	0.362	r=-0.136	0.046	r=0.041	0.726
Age	r=0.137	0.236	r=0.096	0.409	r=-0.038	0.745
Menopause	r=0.163	0.159	r=0.154	0.184	r=0.067	0.57
p-tumor size	r=0.281	0.014	r=0.306	0.007	r=0.256	0.026
Histopathological type	r=0.082	0.479	r=0.059	0.614	r=-0.031	0.791
Nuclear grade	r=0.319	0.004	r=0.333	0.003	r=0.152	0.188
Atypia	r=0.294	0.009	r=0.305	0.008	r=0.152	0.191
Mitosis	r=0.239	0.037	r=0.268	0.019	r=0.181	0.119
pN status	r=0.168	0.146	r=0.153	0.187	r=-0.071	0.54
pT stage	r=0.142	0.222	r=0.163	0.158	r=0.169	0.145
pStage	r=0.254	0.027	r=0.261	0.023	r=0.098	0.57

r; Spearman rank coefficient, SUV1; maximum standardized uptake value 1, RI; retention index, SUV2; maximum standardized uptake value 2, Glut-1; glucose transporter-1, Her2; human epidermal growth factor-2, mTOR; mammalian target of rapamycin, p70S6; p70S6kinase, ERα; estrogen receptorα, ERβ; estrogen receptor β, PR; progesterone receptor, NG; nuclear grade, pN status; pathological N status, pTstage; pathological T stage, pStage; pathological Stage.
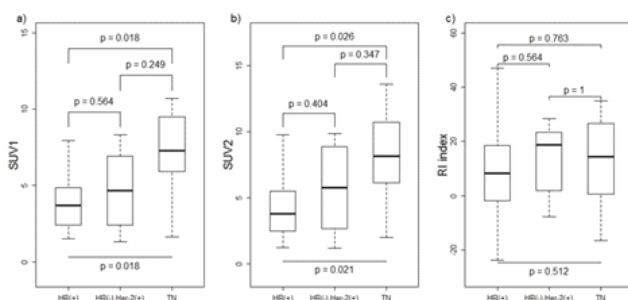

Figure 3. The relationships between PET parameters and breast cancer subtypes [HR (+) subtype, HR (−) Her2 (+) subtype, and TN subtype]. (a) SUV1 and breast cancer subtypes, (b) SUV2 and breast cancer subtypes, and (c) RI and breast cancer subtypes.

der the ROC curves (AUC) and the 95% confidence intervals are presented for +2 and +3 Glut-1 expression, for NG2 and NG3, for ERα negativity, and for pStages II and III in Table 4, as are the results of our comparison of the P-values for the A-UCs of SUV1 and SUV2 relative to those of the RI. Regarding

Glut-1 expression, the ROC curves for SUV1 and SUV2 were far from that of the RI, and the AUC of SUV1 and SUV2 were significantly larger than that of the RI (SUV1:P=0.032, SUV2: P=0.022). For NG, pStage and ERα, the AUC of SUV1 and SUV2 were larger than that of the RI. There were no significant differences among the AUC of the PET parameters.
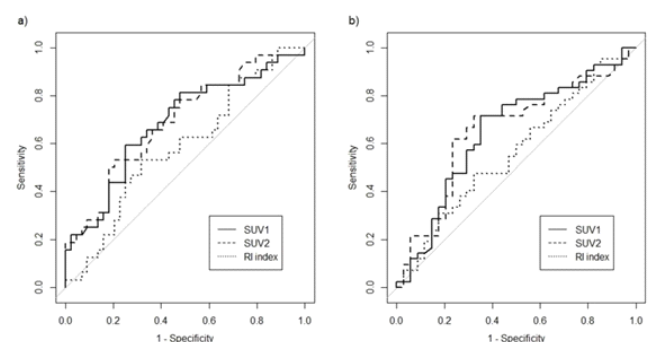
Figure 4. The results of the ROC analysis of the efficiency of each of the three 18F-FDG PET parameters for NG (a) and pStage (b).
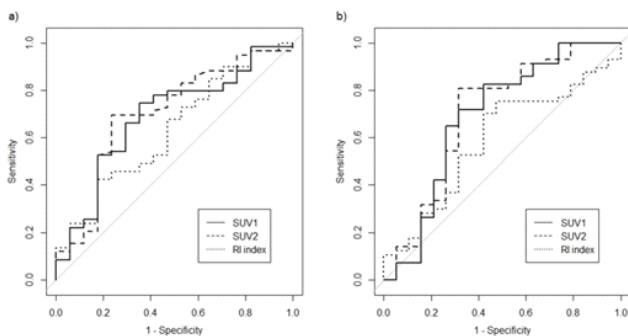
Figure 5. The results of the ROC analysis of the efficiency of each of the three ^{18}F-FDG PET parameters for Glut-1 (a) and ERα (b).

Table 4. The AUC value of SUV1, SUV2 and RI for clinicopathologic parameters.

	P value for pairwise comparison		
Parameters	**AUC**	**95%CI**	**Versus RI**
NG			
SUV1	0.684	(0.560,0.808)	0.199
SUV2	0.69	(0.568,0.812)	0.105
RI	0.583	(0.453,0.714)	Reference
pStage			
SUV1	0.648	(0.521,0.777)	0.273
SUV2	0.654	(0.527,0.782)	0.167
RI	0.563	(0.453,0.714)	Reference
ERα			
SUV1	0.688	(0.542,0.852)	0.302
SUV2	0.695	(0.535,0.856)	0.216
RI	0.582	(0.439,0.737)	Reference
Glut-1			
SUV1	0.693	(0.571,0.815)	0.032
SUV2	0.673	(0.551,0.795)	0.022
RI	0.516	(0.380,0.652)	Reference

NG; Nuclear grade, pStage; pathological Stage, ERα; estrogen receptor α, Glut-1; glucose transporter-1, SUV1; maximum standardized uptake value 1, SUV2; maximum standardized uptake value 2, RI; retention index.

The association between Glut-1 and other biological markers

Glucose transporter-1 had negative correlations with ERα and PR expression, and a positive correlation with ERβ expression (ERα: r=-0.36, P=0.001, PR: r=-0.261, P=0.022, ERβ: r=0.251, P=0.029). Glut-1 was not correlated with mTOR, p7-0S6 or Her2 (mTOR: r=-0.107, P=0.357; p70S6: r=-0.033, P=0.777; Her2: r=-0.027, P=0.814). Glut-1 expression in the TN subtype was significantly higher than those in the HR (+) subtype and HR (−) Her2 (+) subtype [HR (+); P<0.001, HR (−) Her2; P=0.013]. There was no significant difference between HR (+) subtype and HR (−) Her2 (+) subtype regarding Glut-1 expression (P=0.442) (Table 5).

Table 5. The results of immunohistochemical staining of Glut-1expression for breast cancer subtypes.

Subtype	score 0	score 1	score 2	score 3
HR (+) subtype	16	23	16	2
HR (-) Her2 (+) subtype	1	5	3	1
TN subtype	0	2	0	7

Glut-1; glucose transporter-1, HR(+) subtype; hormone receptor positive subtype, HR(-) Her2(+)sub-type; hormone receptor negative, human epidermalgrowth factor-2 positive subtype, TN subtype; triple negative subtype.

Discussion

Our analysis revealed that the SUV1 and SUV2-but not the RI- are positively correlated with Glut-1 values and that the SUVmax rather than the RI could predict the Glut-1 expression. A positive correlation between Glut-1 and ^{18}F-FDG accumulation using single-point imaging has been reported in breast cancer patients [14]. However, no investigations regarding the relationship between Glut-1 and ^{18}F-FDG uptake in breast cancer examined by dual-phase imaging has been reported, to our knowledge. Higashi et al. (2002) suggested that in pancreas cancer patients, high Glut-1 expression was significantly correlated with the SUV1, but not with the RI [15]. In colon cancer patients however, the RI rather than the SUVmax has been reported to be significantly related to the Glut-1 expression, and to predict the Glut-1 expression [16]. The correlations among Glut-1, the SUVmax and the RI may differ by the type of cancer.

In the present study, the SUV1 and SUV2 had significant inverse correlations with ERα, but they were not correlated with ERβ, PR, Her-2, p70S6, or mTOR. The RI was also not correlated with these immunohistochemical factors. Estrogen receptor has two isoforms, ERα and ERβ. Estrogen receptor alpha is a target of hormone therapy, and the increase in ERα expression is crucial in the early stages of breast cancer tumorigenesis. A loss of ERα in breast cancer patients indicates invasiveness and poor prognosis [17]. Estrogen receptor is often co-expressed with ERα, and ERβ expression in breast cancer was reported to be associated with favorable outcomes in women treated with adjuvant tamoxifen, in apocrine breast cancer, and in ERα-negative cancer including TN-BC [18].

The Her2/mTOR signal pathway is one of the important transduction pathways in the growth of breast cancer. Human epidermal growth factor 2 is upstream of this pathway, and p70S6 is downstream of the pathway. Factor p70S6 is related to tumor cell proliferation through protein synthesis [10].

High ^{18}F-FDG accumulation is associated with ER-negative expression, which may be due to ERα negativity, but not ERβ or PR. The Her2/mTOR signal pathway may not contribute to high ^{18}F-FDG uptake in breast cancer. However, other authors have indicated a significant relationship between ^{18}F-FDG uptake and PR or Her2; these correlations are controversial [19, 20]. Moreover, the ^{18}F-FDG uptake in lung cancer was reported to correlate with mTOR [21]. Further studies are needed to clarify the relationship between ^{18}F-FDG uptake and the Her2/mTOR pathway.

In our present study, the SUV1 and SUV2 were significantly positively correlated with p-tumor size, NG, NA, NM, and pStage, but they were not correlated with age, menopausal status, histopathological type, pN status, or pT stage. The RI was positively correlated only with p-tumor size. In addition, higher SUV1 and SUV2 values were observed in the TN subtype than in the HR (+) subtype, whereas the RI was not. Shimoda et al. (2007) reported that the SUV1 and SUV2 had significant positive correlations with the mitotic count, NG and Ki-67, but not with p-N status, histopathological type, tumor size or age [22]. Basu et al. (2008) revealed that high SUV1 and SUV2 values depended on high NG and large tumor size [23]. García Vicente et al. (2013) suggested that the SUV1 and SUV2 in Her2-type and TNBC patients were significantly higher than those in luminal A-type patients and luminal B-type patients, but the RI was not [24].

Moreover, in the present study, the SUV1 and SUV2 had significant correlations with Glut-1 and ERα, whereas the RI did not. Our data suggest that the SUVmax rather than the RI is associated with immunohistochemical and clinicopathological prognostic factors. However, some authors have suggested that the RI (rather than the SUVmax) reflects the clinicopathological factors because the RI is associated with TNBC, the tumor size, stage, NG and Her2 [23, 25]. The relationships between immunohistochemical and clinicopathological prognostic factors and the SUVmax or RI are controversial, and these issues should be clarified in future studies.

We observed that Glut-1 was inversely correlated with ERα and PR, and positively correlated with ERβ. Glut-1 was not correlated with the Her2/mTOR signal pathway. Regarding the breast cancer subtypes, significant high Glut-1 expression was observed in the TN subtype rather than the HR (+) subtype or HR (-) Her2 (-) subtype. When hypoxia occurs in breast cancer cells, the expressions of ERα and PR are decreased via a proteasome-dependent pathway [26]. In addition, hypoxia was followed by an increase in Glut-1 and ERβ expression, and Glut-1 expression was increased in poorly differentiated breast cancer and associated with high proliferative activity, increased invasiveness, aggressive behavior and TNBC, but not with Her2 expression [27, 28]. Our present findings suggest that a patient's steroid hormone expression status has a greater influence on Glut-1 expression than the Her2/mTOR signal pathway.

Our resultant data show that the SUVmax may be more useful than the RI for predicting the aggressiveness of breast cancer. Breast cancer patients with a high SUVmax may have resistance to hormone therapy, and chemotherapy or molecular target therapy may be necessary for these patients. Glut-1 is considered to be a factor of molecular target therapy, and the usefulness of a Glut-1 inhibitor has been reported in breast cancer patients [27]. If a Glut-1 inhibitor is used as molecular target therapy to breast cancer patients, the SUVmax may be useful for identifying the appropriate patients and evaluating the therapeutic effect of the Glut-1 inhibitor because the SUVmax predicts the Glut-1 expression level. Clinically, the SUVmax may be a more promising marker than the RI for deciding the management of therapy.

Prone breast PET/CT imaging was performed, because this imaging is more useful for detecting breast cancer than supine-position PET imaging due to its better delineation of lesions by expansion of the breast parenchyma, as well as its higher influx of ^{18}F-FDG to the breast [12, 29]. In addition, we performed delayed prone PET/CT imaging at 125min after the tracer administration. As with most other cancers, the majority of breast malignancies show a gradual increase in SUVs over time after ^{18}F-FDG injection [5]. Boerner et al. (19-99) suggested that the tumor contrast in breast cancer is even more improved by starting the PET acquisition at 180 min rather than 90min after the tracer administration [30]. However, it is difficult to perform the delayed PET imaging at 180min after tracer administration clinically because the PET/CT examination is time consuming. Basu et al. (2008) have investigated the relationship between ^{18}F-FDG uptake and clinicopathological factors in breast cancer patients using dual-phase PET imaging within 120min after the administration of ^{18}F-FDG, have suggested that high SUV1 (63min after injection) and SUV2 (101min after injection) were associated with TNBC and high tumor grade [23]. In the present study, the results of our analysis of the correlations between the SUV1 and both immunohistochemical and clinicopathological risk factors are almost the same as those for the SUV2. The RI did not correlate with other immunohistochemical and clinicopathological risk factors except for the p-tumor size. Recently, Garcia-Vicente et al. (2017) have investigated relationship between biological characteristics and molecular phenotypes and ^{18}F-FDG PET dual point imaging (PET-1; 1hour, PET-2; 3hours) using volumetric parameters and SUV, and they have suggested that most of PET-derived parameters showed high association with molecular factors of breast cancer in 67 local advanced breast cancer patients [31]. Delayed ^{18}F-FDG PET/CT imaging may not give additional information about the clinicopathological and immunohistochemical prognostic factors of breast cancer. The clinically optimal time and usefulness for delayed ^{18}F-FDG PET imaging should be investigated in the future.

Our study has some limitations. First, the number of patients was relatively small, and hypoxia inducible growth factor-1alpha (HIF-1α) was not investigated. However, in breast cancer patients, HIF-1α has been reported to be associated with Glut-1 upregulation [13]. Second, we could not analyze the prognosis of the patients because the numbers of recurrent patients and deaths were low, and 65 of the 76 patients (83%) were below stage IIA. The number of Stage IIA patients was small. Breast cancer patients who underwent neoadjuvant chemotherapy were excluded be-

cause we performed IHC to evaluate the Glut-1, mTOR and p70S6 expressions using operatively extracted specimens. The main purposes of this study were to investigate which PET parameters (the SUVmax or the RI) are suitable for predicting the degree of malignancy, and to elucidate which molecular markers contribute to the ^{18}F-FDG uptake mechanism of breast cancer. Further investigations of prognosis using these PET parameters and both immunohistochemical and clinicopathological prognostic factors should be performed in larger patient populations.

In conclusion, Glucose transporter-1, ERα negativity and NG might affect the high ^{18}F-FDG uptake mechanism of breast cancer, rather than PR, ERβ and the Her2/mTOR signal pathways. The SUVmax might be more useful than the RI for predicting the Glut-1 expression and the aggressiveness of breast cancer.

Bibliography

1. Torre LH, Bray F, Siegel RL et al. Global cancer statics, 2012. *Cancer J Clin* 2015; 65: 87-108.
2. Zhang C, Wang S, Israel HP et al. Higher locoregional recurrence rate for triple-negative breast cancer following neoadjuvant chemotherapy, surgery and radiotherapy. *Springerplus* 2015; 4: 386.
3. Ahn SG, Lee M, Jeon TJ et al. ^{18}F-flurodeoxyglucose positron emission tomography can contribute to discriminate patients with poor prognosis in hormone receptor positive breast cancer. *PLoS One* 2014; 9: e105905.
4. Groheux D, Majdoub M, Sanna A et al. Early Metabolic Response to Neoadjuvant Treatment: FDG PET/CT Criteria according to Breast Cancer Subtype. *Radiology* 2015; 277: 358-71.
5. Kumar R, Loving VA, Chauhan A et al. Potential of dual-time-point imaging to improve breast cancer diagnosis with ^{18}F-FDG PET. *J Nucl Med* 2005; 46: 1819-24.
6. Imbriaco M, Caprio MG, Limite G et al. Dual-time-point ^{18}F-FDG PET/CT versus dynamic breast MRI of suspicious breast lesions. *Am J Roentgenol* 2008; 191: 1323-30.
7. Shimizu K, Okita R, Saisho S et al. Clinical significance of dual-time-point ^{18}F-FDG PET imaging in resectable non-small cell lung cancer. *Ann Nucl Med* 2015; 29: 854-60.
8. Abgral R, Le Roux PY, Rousset J et al. Prognostic value of dual-time-point ^{18}F-FDG PET-CT imaging in patients with head and neck squamous cell carcinoma. *Nucl Med Commun* 2013; 34: 551-6.
9. Yoon HJ, Kim SK, Kim TS et al. New application of dual point ^{18}F-FDG PET/CT in the evaluation of neoadjuvant chemoradiation response of locally advanced rectal cancer. *Clin Nucl Med* 2013; 38: 7-12.
10. Hernandez-Aya LF, Gonzalez-Angulo AM. Targeting the Phosphatidylinositol 3-Kinase Signaling Pathway in breast cancer. *Oncologist* 2011; 16: 404-14.
11. Sobin LH, Wittekind Ch; In (International Union Against Cancer |UICC|), eds. *TNM classification of malignant tumors. 6th ed. Baltimore, MD: Wiley-Liss*; 2002.131-41.
12. Kaida H, Ishibashi M, Fujii T et al Improved breast cancer detection of prone breast fluorodeoxyglucose-PET in 118 patients. *Nucl Med Commun* 2008; 29: 885-93.
13. Robbins P, Pinder S, de Klerk N et al. Histopathological grading of breast carcinoma: a study of interobserver agreement. *Hum Pathol* 1995; 26: 873-9.
14. Bos R, van der Hoeven JJ, van der Wall E et al. Biologic Correlation of ^{18}F-fluorodeoxyglucose uptake in human breast cancer measured by positron emission tomography. *J Clin Oncol* 2002; 20: 379-87.
15. Higashi T, Saga T, Nakamoto Y et al. Relationship between retention index in dual phase ^{18}F-FDG PET, and hexokinase-II and glucose trasporter-1 expression in pancreas cancer. *J Nucl Med* 2002; 43: 173-80.
16. Lee JH, Lee WA, Park SG et al. Relationship between dual time point FDG-PET and Immunohistochemical Parameters in Preoperative Colorectal Cancer: Preliminary Study. *Nucl Med Mol Imaging* 2012; 46: 48-56.
17. Cooper C, Lin GY, Niu YL et al. Intermittent hypoxia induces proteasome-dependent down-regulation of estrogen receptor α in human breast carcinoma. *Clin Cancer Res* 2004; 10: 8720-27.
18. Honma N, Horii R, Iwase T et al. Clinical importance of estrogen receptor-beta evaluation in breast cancer patients treated with adjuvant tamoxifen therapy. *J Clin Oncol* 2008; 26: 3727-34.
19. Kim BS, Sung SH. Usefulness of ^{18}F-FDG uptake with clinicopathologic and immunohistochemical prognostic factors in breast cancer. *Ann Nucl Med* 2012; 26: 175-83.
20. Osborne JR, Port E, Gonen M et al. ^{18}F-FDG PET of locally invasive breast cancer and association of estrogen receptor status with standardized uptake value; microarray and immunohistochemical analysis. *J Nucl Med* 2010; 51: 543-50.
21. Kaira K, Serizawa M, Koh Y et al. Biological significance of ^{18}F-FDG uptake on PET in patients with non-small cell lung cancer. *Lung Cancer* 2014; 83: 197-204.
22. Shimoda W, Hayashi M, Murakami K et al. The relationship between FDG uptake in PET scans and biological behavior in breast cancer. *Breast cancer* 2007; 14: 260-73.
23. Basu S, Chen W, Tchou J et al. Comparison of triple negative and estrogen receptor positive/progesterone receptor-positive/Her2-negative breast carcinoma using quantitative fluorine-18 fluorodeoxyglucose/positron emission tomography imaging parameters: a potentially useful method for disease characterization. *Cancer* 2008; 112: 995-1000.
24. García Vicente AM, Soriano Castrejón Á, León Martín A et al. Molecular subtype of breast cancer; metabolic correlation with ^{18}F-FDG PET/CT. *Eur J Nucl Med Mol Imaging* 2013; 40: 1304-11.
25. García Vicente AM, Castrejón ÁS, Relea Calatayud F et al. ^{18}F-FDG retention index and biologic prognostic parameters in breast cancer. *Clin Nucl Med* 2012; 37: 460-6.
26. Cooper C, Liu GY, Niu YL et al. Intermittent hypoxia induces proteasome-dependent down-regulation of estrogen receptor α in human breast carcinoma. *Clin Cancer Res* 2004; 10: 8720-7.
27. Hussein YR, Bandyopadhyay S, Semaan A et al. Glut-1 expression correlates with basal-like breast cancer. *Trasitional Oncol* 2011; 4: 321-7.
28. Koo JS, Jung W. Alteration of REDD1-mediated mammalian target of rapamycin pathway and hypoxia-inducible factor-1α regulation in human breast cancer. *Pathobiology* 2010; 77: 289-300.
29. Magometschnigg HF, Baltzer PA, Fueger B et al. Diagnostic accuracy of ^{18}F-FDG PET/CT compared with that of contrast-enhanced MRI of the breast at 3T. *Eur J Nucl Med Mol Imaging* 2015; 42: 1656-65.
30. Boerner AR, Weckesser M, Herzog H et al. Optimal scan time for fluorine-18 fluorodeoxyglucose positron emission tomography in breast cancer. *Eur J Nucl Med* 1999; 26: 226-30.
31. Garcia-Vicente AM, Pérez-Beteta J, Pérez-García VM et al. Metabolic Tumor Burden Assessed by Dual Time Point ^{18}F-FDG PET/CT in Locally Advanced Breast Cancer: Relation with Tumor Biology. *Mol Imaging Biol* 2017; 19: 636-44.